

pubs.acs.org/JACS Article

How Hole Injection Accelerates Both Ion Migration and Nonradiative Recombination in Metal Halide Perovskites

Chuan-Jia Tong, Xiaoyi Cai, An-Yu Zhu, Li-Min Liu,* and Oleg V. Prezhdo*



Cite This: J. Am. Chem. Soc. 2022, 144, 6604–6612



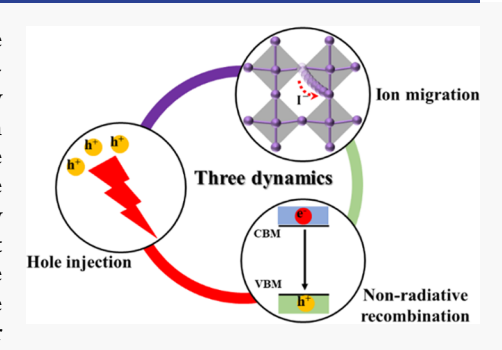
ACCESS

Metrics & More

Article Recommendations

s Supporting Information

ABSTRACT: Ion migration, hole trapping, and electron—hole recombination are common processes in metal halide perovskites. We demonstrate using ab initio non-adiabatic molecular dynamics and time-domain density functional theory that they are intricately related and strongly influence each other. The hole injection accelerates ion migration by decreasing the diffusion barrier and shortening the migration length. The injected hole also promotes the nonradiative charge recombination by strengthening electron—phonon interactions in the low-frequency region and prolonging the quantum coherence time. The synergy stems from the soft perovskite lattice and response of the valence band maximum to the Pb—I lattice distortion induced by the hole. This work provides important insights into the influence of ion mobility and hole injection on the performance of perovskite solar cells and suggests that high concentration of holes should be avoided.



1. INTRODUCTION

Ion migration is a ubiquitous process in organic—inorganic halide perovskites, such as ${\rm CH_3NH_3PbI_3}$ (MAPbI₃), facilitated by their soft crystalline lattice and has been an important topic of research in the recent years. Among all the ions, the halide (iodide) ion has been demonstrated the most mobile, exhibiting the lowest activation energy barrier. The movement of halide ions can even be seen visually on a macroscopic scale in experiments. The iodine migration has been reported to play multiple detrimental roles, such as inducing the strong current—voltage hysteresis $^{14-17}$ and promoting the nonradiative electron hole (e—h) recombination. Thus, it should be minimized to improve the overall performance of perovskite solar cells.

The movement of iodide ions was visualized by an electrochemical hole injection in the work²³ of Samu et al. Kamat's group²⁴ found that localization of holes in perovskites induces instability and promotes iodide moving toward grain boundaries. Xiao et al.²⁵ observed that the hole injection can improve the radiative recombination intensity of perovskite light-emitting diodes. These experimental findings raise several fundamental questions. First, it is important to establish at the atomistic level why the injected holes accelerate the iodine migration. This information can be used to control the migration and design compositions and structures that minimize ion segregation. Second, it is important to understand how the hole injection and the ion migration influence the charge carrier lifetimes. Charge carrier lifetime is one of the key properties governing solar cell efficiencies. If the hole injection increases the radiative recombination, 25 very likely, it affects the nonradiative recombination as well, and nonradiative recombination is the main source of charge carrier

and current and voltage losses in solar cells in general. In order to answer these questions and to gain clear atomistic insights into the processes that govern efficiencies of perovskite solar cells and other optoelectronic devices, atomistic simulations of perovskite structure and equilibrium and non-equilibrium molecular quantum dynamics are required.

In this work, we use ab initio non-adiabatic molecular dynamics (NAMD) together with both time-independent and real-time time-dependent density functional theory (DFT) to study iodine migration and e-h recombination in the holeinjected and hole-free MAPbI₃ perovskite. Our simulations show that (1) hole injection can accelerate iodine diffusion by (i) decreasing the diffusion barrier in the XY plane and (ii) shortening the migration length in the vertical (Z) direction and (2) hole injection can accelerate the nonradiative recombination based on three reasons (i) it promotes ion diffusion and ion diffusion accelerates e-h recombination; (ii) it extends the quantum coherence time by enlarging the overlap between the wave functions of the valence band maximum (VBM) and the conduction band minimum (CBM); and (iii) it enhances electron-phonon interactions. The reported results provide valuable fundamental insights into how hole injection accelerates both ion diffusion and e-h recombination, demonstrating that high hole concentration

Received: February 26, 2022 Published: April 1, 2022





can be detrimental to the overall performance of metal halide perovskite solar cells and should be avoided.

2. SIMULATION METHODOLOGY

The DFT calculations were performed using the Gaussian function double- ζ polarized basis sets (m-DZVP)²⁶ to describe valence electrons, as implemented in the CP2K/Quickstep²⁷ package. The core electrons were described with the normconserving Goedecker-Teter-Hutter²⁸ pseudopotential. A 500 Ry energy cutoff was set for the real space grid throughout the whole study. To save the computational cost for a 2 \times 2 \times 2 supercell containing 384 atoms, the exchange-correlation energy was calculated with the Perdew-Burke-Ernzerhof²⁹ functional, which performed well with the ground-state and NAMD calculations in the previous MAPbI₃-type perovskite studies.^{30–34} The DFT-D3 method^{35,36} was used to describe long-range van der Waals interactions. The diffusion pathways and the activation energies were obtained with the climbing image nudged elastic band (CI-NEB)^{37,38} method. Seven images were distributed along the diffusion pathway connecting the initial and final states, with each image fully optimized during the NEB calculations. NAMD were performed with the decoherence-induced surface hopping (DISH)³⁹ approach, as implemented in the PYXAID^{40,41} package. The method was used successfully to simulate excited-state dynamics in a variety of perovskite systems and other materials, 42-50 and more theory details can be found in the previous publication.

3. RESULTS AND DISCUSSION

3.1. Description of Introducing the Hole. Figure 1a shows the initial tetragonal MAPbI₃ structure that is energeti-

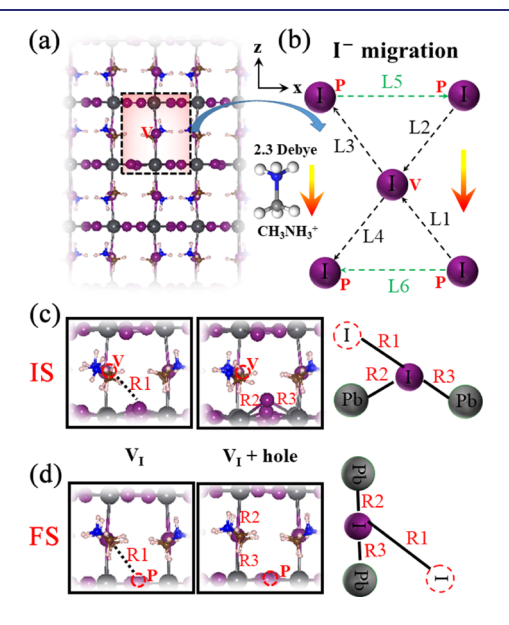


Figure 1. (a) Side view of the tetragonal MAPbI₃. The colored arrow shows direction of the built-in dipole induced by the MA⁺ molecule. (b) Scheme of the I⁻ ion migration mechanism in MAPbI₃, projected onto the XZ plane, as highlighted by the dashed frame in (a). The dashed arrows demonstrate different diffusion pathways, referred to as L1 to L6. (c) Initial and (d) final configurations of the diffusion pathway L1. Left: iodine vacancy (V_I) without the hole. Middle: V_I with one hole. Right: schematic of the Pb–I lattice around the migrating iodine. (Dark gray—lead; purple—iodine; brown—carbon; blue—nitrogen; white—hydrogen.)

cally favorable and induces less current-voltage hysteresis, as reported in the previous work.⁵¹ In addition to the stability and reduced hysteresis, there are two more key observations. First, the iodine atoms in MAPbI₃ are not equivalent. They prefer locating at vertical (V) sites, whereas iodine vacancies prefer locating at parallel (P) sites. Second, there are different iodine migration pathways in MAPbI₃ depending on the sites and the dipoles induced by MA molecules, as shown in Figure 1b. With reference to the previous work, 51 we consider one hole in the MAPbI₃ perovskite. Normally, the hole is introduced by adding a positive charge to the system, with the spurious interactions of the periodically replicated charge screened by a uniform neutralizing background. 52 However, due to the limit of the simulation cell size, the artificial image charge will have an over-influence on the system by introducing an extra unphysical electric field. Here, in the iodine-vacant perovskite, it does not introduce any gap states but decreases the band gap by about 0.1 eV. More details can be seen in Figure S1a,b in Supporting Information. Such a variation of the band edge properties can artificially influence the nonradiative recombination. A recent report⁵³ has established the importance of a proper description of electron-phonon interactions near the band edges.

To avoid the errors that can stem from modeling charged systems under periodic boundary conditions, we consider an alternative method to introduce the hole. Namely, we remove two MA molecules far from the iodine vacancy, based on the three reasons. First, iodine atoms in MAPbI₃ carry a -1 charge, whereas MA⁺ cations carry a +1 charge. Removing MAI creates an iodine vacancy without changes to oxidation states of any species. Removing a second neural MA removes an electron because MA can be viewed as MA+ plus an electron, thus creating a model for the hole. Second, MA molecules do not contribute to band edge states. Removing two of them does not alter the electronic properties around the edges and the band gap remains unchanged, as confirmed in Figure S1c,d in Supporting Information. Third, the non-adiabatic coupling (NAC) responsible for the nonradiative charge recombination is generated by the Pb-I lattice and has little contribution from the MA⁺ cations. The soft Pb-I lattice introduces efficient low-frequency phonons^{54,55} and contributes to polaron formation. A similar method of modeling an electron injection was used in the Fe₂O₃ study, namely an extrinsic defect Si was used to transfer one extra electron to Fe^{3+.58} Similar methods of introducing a hole have been reported in other DFT simulations, by doping with low-valence atoms or by adsorption of hydroxyl radicals on the surface. 59,60

3.2. Influence of Hole Injection on Iodine Diffusion. The defect diffusion pathways have been simulated with the NEB method, and the calculated activation energy barriers are summarized in Table 1. The barriers obtained in the presence of a hole are compared with those for the hole-free perovskite. The data show that the iodine migration barriers decrease when there is a hole in the system. Especially, when the migration occurs between the P sites in the XY plane, L5 and L6, the energy barriers drop from 0.38 eV down to 0.13 eV. Such a dramatic, threefold decrease of the barrier height indicates that the iodine migration is very sensitive to the injected hole. The low barriers, on the order of 0.1 eV, rationalize the movement of iodines upon hole injection observed in the experiment. 23,24 Although the barriers in the vertical (Z) direction, L1–L4, do not exhibit a significant change upon the hole injection, the changes are around 0.05

Table 1. Energy Barriers (E_b) for Iodine Diffusion along Different Pathways, as Shown in Figure 1b, in the Hole-Injected and Hole-Free Perovskites^a

pathway	hole-injected	hole-free ^b
L1	0.05	0.06
L2	0.29	0.33
L3	0.37	0.32
L4	0.45	0.65
L5	0.14	0.38
L6	0.13	0.38
arris W bosts from		

^aUnit: eV. ^bData from ref 51.

eV in most cases. The injection can influence the ion diffusion in other ways, for instance, by shortening the length of migration between the initial and final vacancy locations, which can be established by comparing the optimized configurations. The only exception occurs in L3, as its migration barrier increases after the hole injection. The reason is related with a more significant structural distortion. The distortion in this case involves both Pb–I and MA species, see Figure S2 and detailed analysis in Supporting Information. The barriers for the other diffusion pathways decrease, and the main conclusion holds.

In addition to changing the ion diffusion barriers, the hole injection causes significant structural modifications. We consider the initial structure (IS) and the final structure (FS) for pathway L1 as an example. Figure 1c,d shows the configurations around the migrating iodine and compares the structures with and without the hole. A large difference is seen in L1-IS, Figure 1c, arising mainly from a 1.35 Å buckle in the vertical direction caused by the injected hole. The upward shifted iodine induces a serious distortion in the Pb-I lattice. These results are consistent with the findings reported for CH₃NH₃Br₃, showing that a positive added charge induces a large structural change in the Pb-Br lattice.⁵⁶ As for L1-FS, Figure 1d, no obvious difference can be identified visually. To clearly describe the configuration difference between the holeinjected and hole-free perovskites, both containing an iodine vacancy V_I, we present schematics in the rightmost part of Figure 1c,d and select several internal parameters. They are the iodine migration length R1, the two Pb-I bond lengths R2 and R3, and the bond angle Pb-I-Pb between the bonds R2 and R3. The data are collected in Table 2.

The data of Table 2 confirm that a much more significant structure distortion occurs in L1-IS than L1-FS, namely when V_I is located at the V site. V_I is more energetically favorable on the P site. Thus, when the hole is injected into the perovskite, it introduces further lattice instability and drives V_I (iodine) from site V (P) to P (V). As a consequence, the injected hole

Table 2. Internal Parameters of the L1-IS and L1-FS Structures in the Perovskite Systems without and with the Injected ${\rm Hole}^a$

	R1, R2, R3 in L1-IS (Å)	Pb-I-Pb in L1-IS (deg)	R1, R2, R3 in L1-FS (Å)	Pb-I-Pb in L1-FS (deg)
V_{I}	4.22, 3.16, 3.16	156.99	4.53, 3.27, 3.25	170.71
V _I + hole	3.62, 3.20, 3.23	131.27	4.51, 3.30, 3.27	170.52

^aThe parameters are defined in Figure 1c,d. The Pb–I–Pb angle corresponds to R2–I–R3.

drastically shortens the I-V_I distance, that is, the migration length R1, by around 0.6 Å compared with the hole-free V_I perovskite. At the same time, the injected hole does not change the Pb-I bond lengths by much. The variations in R2 and R3 are no more than 0.07 Å. The injected hole also has a strong influence on the Pb-I-Pb angle, which decreases by 25.72° because the iodine moves out. The result agrees well with the recent work of de Angelis and co-workers, of who found that a positive charge decreases the Pb-I-Pb angle in the equatorial plane. As for L1-FS, the iodine is already located at the stable V site and therefore there is almost no structure distortion even after the hole injection. The variations in R1, R2, R3, and Pb-I-Pb are small, 0.02, 0.03, 0.02 Å, and 0.19°, respectively, and can be neglected. It can be concluded that the injected hole can accelerate the iodine migration by shortening the migration length along the Z direction. The inherent softness of the perovskite lattice⁶² is the fundamental reason for this structural instability.

We have also collected the same parameters when migration occurs in the XY plane (L5) and summarized the results in Table 3. This time, we find that when the $V_{\rm I}$ is located at the P

Table 3. Internal Parameters of L5-IS and L5-FS in the Perovskite Systems^a

	R1, R2, R3 in L5-IS (Å)	Pb-I-Pb in L5-IS (deg)	R1, R2, R3 in L5-FS (Å)	Pb-I-Pb in L5-FS (deg)
$V_{\rm I}$	4.29, 3.18, 3.13	152.59	4.15, 3.09, 3.31	177.98
V _I + hole	4.27, 3.18, 3.12	149.80	4.17, 3.04, 3.32	177.85

^aThe parameters are defined in Figure 1 and Table 2.

site, both the initial and final configurations are very stable, and the injected hole can only slightly change the Pb-I-Pb angle (1.70° in L5-IS) and the migration length R1 (0.02 Å). The variation in the L5-FS configuration is very small, and all internal parameters almost remain unchanged, which indicates that the hole injection does not induce a Pb-I lattice distortion when V_I is at the P site. Therefore, the main mechanism of the hole promoting the ion diffusion here is the much lower migration barrier, as shown in Table 1. The different hole-assisted migration mechanisms, depending on the V_I location, are discovered in this work for the first time. The same conclusions can be achieved by introducing the positive charge as well, see Tables S1-S3 in Supporting Information, once again proving the validity of our novel approach for introducing the hole into metal halide perovskites without the addition of a positive charge.

3.3. Influence of Hole Injection on Charge Recombination. Having demonstrated that the injected hole can accelerate iodine migration, we investigate whether the hole injection influences the nonradiative charge recombination, either directly by changing the electronic properties of the band edge states and electron-vibrational coupling, or indirectly by accelerating the iodine migration, which in turn can influence the charge recombination. The latter type of synergy has been seen for the neutral vacancy in the previous study, which has established that defect migration introduces a trap state into the fundamental energy gap, thereby accelerating the charge recombination by an order of magnitude. One can expect that the strong distortion of the Pb–I lattice can alter perovskite electronic properties. For example, Zhou et al.⁶³ have found recently that the Pb–I–Pb

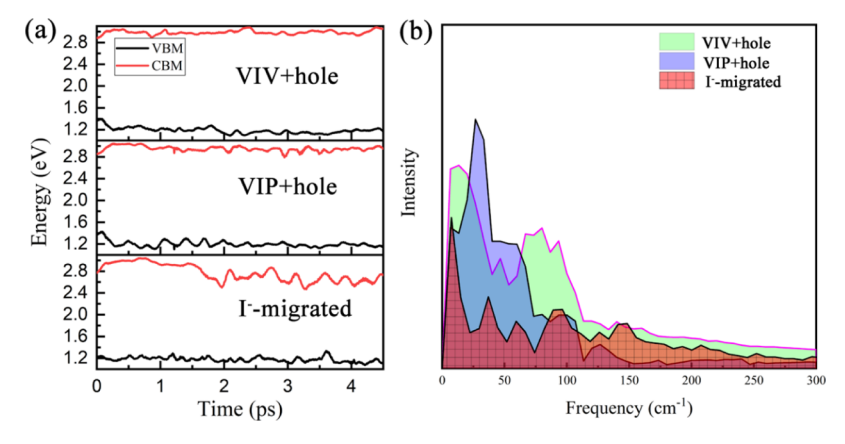


Figure 2. (a) Evolution of the VBM and CBM energies for hole-injected VIV, hole-injected VIP, and hole-free I-migrated MAPbI₃ perovskites, from top to bottom, respectively. (b) Fourier transforms of the autocorrelation function of the VBM energy in the three systems.

angle is the third most important structural parameter that can affect the electronic properties and NAC. Miyata et al. 56 have established that the Pb–Br–Pb deformation modes influence the charge carrier recombination by introducing large polarons. Many experimental and theoretical works have reported that the bending and stretching of Pb–I–Pb generate low-frequency phonons, which play vital roles in the nonradiative e–h recombination in MAPbI $_3$ and related perovskites. Based on these reports, we investigate the influence of the injected hole on the nonradiative charge recombination next.

Because the iodine vacancy can be present in nonequivalent sites, we consider both the vacancy in V (VIV) site, namely the L1-IS, and the vacancy in P (VIP) site, namely the L5-IS, as shown in Figure 1. Before investigating quantum dynamics of the recombination process, we analyze the static, 0 K electronic structures, see Figure S1c,d. The projected density of states indicates that the hole injection does not introduce mid-gap states at 0 K. The previous first-principles MD simulation has shown that a deep trap state is generated once a Pb-Pb dimer is formed during iodine migration at an ambient temperature. However, because iodine migration involves significant energy barriers, it cannot be easily captured in a few picosecond MD trajectory and therefore it is not seen in our MD simulation. Importantly, the properties of the systems near the potential energy minima still change significantly in the presence of the injected hole. Figure 2a exhibits evolution of the VBM and CBM energies, comparing the hole-injected and hole-free perovskites. A particularly strong fluctuation occurs in the CBM in the hole-free system, bottom panel. Such fluctuation is a precursor to the formation of the Pb-Pb dimer that occurs during the iodine migration. 18 In comparison to the CBM, the VBM fluctuates much less in the hole-free perovskite. The situation reverses when the hole is injected. Both VIV and VIP show a relatively larger fluctuation in the VBM than the CBM. The VBM of MAPbI₃ is dominated by interacting Pb-6s and I-5p orbitals, whereas the CBM arises from the Pb-6p orbital. Therefore, the VBM is more sensitive than the CBM to the distortion of Pb-I lattice that influences overlap of the Pb-6s and I-5p orbitals. Similar results have been established for MAPbBr₃ as well.⁵⁶ In addition, the absolute energy levels of the band edges upshift when the hole is injected. Once again, the difference is larger in the VBM, around 0.2 eV, compared to the CBM, about 0.06 eV. The upshift is ascribed to changes of the electrostatic potential.

Fluctuations in the energies of the band edge states are due to coupling to phonons that can govern the nonradiative e-h recombination. To provide additional insights into the electron-phonon interactions, we calculate Fourier transforms of the autocorrelation functions of the fluctuations in the VBM for all three perovskite systems, as shown in Figure 2b. The frequencies of the dominant phonon modes are below 150 cm⁻¹, which agrees well with the previous studies. 54,64 These low-frequency phonons are due to motions of the inorganic Pb-I lattice, including bending and stretching. The signal intensity is stronger in the hole-injected systems compared with the hole-free perovskite, indicating stronger electronphonon interactions. The interactions are enhanced in the presence of the hole because of distortion of the soft Pb-I lattice, as discussed above. A similar finding⁵⁶ has been reported for MAPbBr₃, that is, injection of a positive charge (hole) can introduce a stronger electron-phonon coupling than injection of a negative charge (electron). Generally, the soft Pb-I lattice responds to injected charges by creating polarons. In particular, by distorting the Pb-I lattice the injected hole intensifies low-frequency phonon modes, which in turn can promote the nonradiative charge recombination.

In order to determine whether the injected hole changes the timescale and mechanism of the nonradiative charge recombination, we perform NAMD simulations using the DISH approach. ^{39–41} Figure 3a–c depicts decay of the excitedstate population due to the charge recombination. Iodine migration can accelerate the e-h recombination depending on the position of the iodine atom. 18 Therefore, we separate the NAMD data into three steps as shown in Figure 3c. Step I is prior to the migration. It is equivalent to a V_I in MAPbI₃ near equilibrium. Interestingly, VIP also shows a stepwise population decay, Figure 3b, which is similar to the first two steps in the I-migrated perovskite, Figure 3c. This is because the L5 iodine migration pathway remains almost unchanged in VIP, as detailed above. The injected hole only decreases the diffusion barrier, which makes the recombination behavior close to the early stage of that in the I-migrated perovskite, although the migration is not complete. Then, step I can also be regarded as the recombination in the hole-injected MAPbI₃ without migration, and the estimated e-h lifetime is 0.089 ns, shorter than that (0.12 ns) of the hole-free perovskite. As for VIV, Figure 3a, it does not show a stepwise behavior. Instead, the standard single component decay with an estimated carrier lifetime of 0.058 ns is obtained. This can be understood as

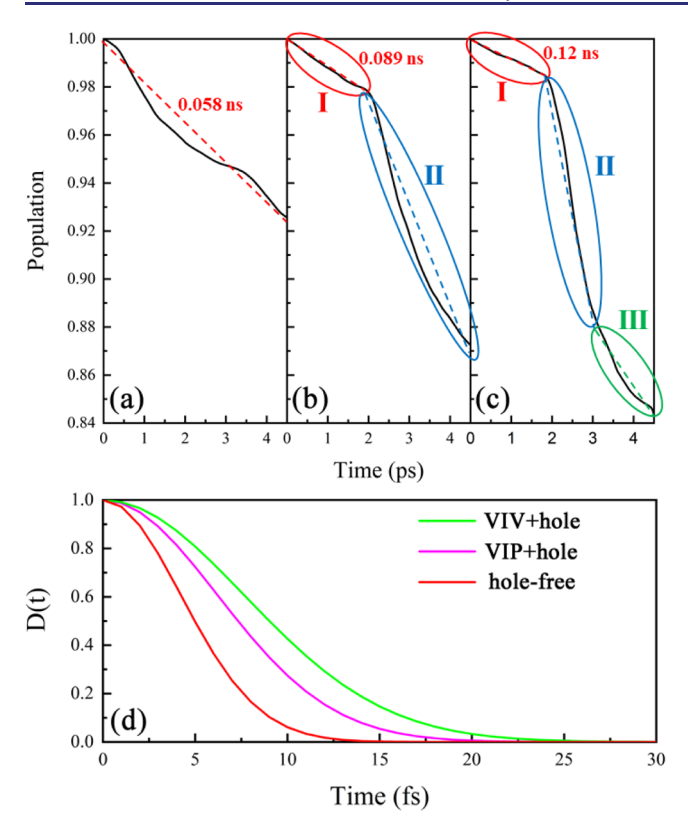


Figure 3. Decay of the excited-state population in (a) hole-injected VIV, (b) hole-injected VIP, and (c) hole-free I-migrated MAPbI₃ perovskites. The colored dashed lines show linear fits. (d) Pure-dephasing functions of the three perovskite systems.

well. The migration distance in L1 has been shortened, which makes the diffusion process different. As a result, the recombination behavior is also different when no iodine migration takes place. In brief, by comparing the data in Figure 3a-c, it can be concluded that the charge carrier lifetime is notably shortened due to the injected hole. To establish the reasons behind the accelerated recombination in the hole-injected perovskites, we analyze the factors that influence the nonradiative transitions.

3.4. Analysis of Electronic Structure and Quantum Coherence. The nonradiative e—h recombination depends on the band gap, the NAC, and the decoherence/pure-dephasing time between the initial and final states. Generally, smaller band gap, stronger NAC, and longer pure-dephasing time lead to faster e—h recombination. Because the band gap remains almost the same after the hole injection, the reduced e—h lifetimes in the hole-injected MAPbI₃ may be attributed to the stronger NAC or longer pure-dephasing time. These factors are summarized in Table 4. The NAC is slightly larger in the hole-injected systems, in particular in VIV. The larger NAC arises

Table 4. Key Properties of the Three Different Perovskites in NAMD Simulations, Including Average Absolute NAC, Pure-Dephasing Time, Nonradiative Lifetime, and Overlap between Charge Densities of the Initial and Final States

	NAC (meV)	dephasing (fs)	lifetime (ns)	overlap
VIV + hole	3.07	8.89	0.058	0.070
VIP + hole	2.42	7.52	0.089	0.067
hole-free VI	2.35	5.23	0.12	0.011

from stronger coupling of the electronic subsystem to the phonon modes in the hole-injected system, Figure 2b. Participation of the higher frequency modes favors larger NAC because the NAC is proportional to the atomic velocity, 40 and the velocity is higher for higher frequency motions at a fixed kinetic energy, which is determined by temperature.

The most significant factor that differs among the three perovskite systems is the pure-dephasing time, Figure 3d and Table 4. Such difference is rare in the previous perovskite reports. 65-67 The pure-dephasing time is the shortest in the hole-free iodine-vacant perovskite, 5.23 fs. The pure-dephasing time becomes considerably 44-70% longer after the hole injection, 7.52 fs for VIP and 8.89 fs for VIV. The puredephasing time depends on the correlation between the phonon-driven fluctuations of the initial and final state energies, and the correlation between the states depends on the overlap of their charge densities. The VBM and CBM wave functions are spatially separated in pristine metal halide perovskites. This is one of the key reasons why the perovskites exhibit large charge-carrier lifetimes. The overlap between the VBM and CBM charge densities remains small even in the presence of iodine vacancies, as confirmed by the charge density distribution of the relevant orbitals reported in the previous work.⁵⁴ To quantify the overlap between electrons and holes, we calculated the following integral between the VBM and CBM charge densities

$$\int |\Psi_{\rm VBM}(r)| |\Psi_{\rm CBM}(r)| {\rm d}^3 r$$

where Ψ_i is the wave function of the *i*th orbital satisfying $\int |\Psi_i|^2 \mathrm{d}^3 r = 1$. The overlap integral of the hole-free perovskite is small because the VBM and CBM charge densities are well separated, Figure 4. In comparison, the overlap increases when a hole is injected by over a factor of 6. The larger e—h overlap results in more correlated fluctuations and longer pure-dephasing times, Table 4.

Figure 4 demonstrates that hole injection changes the properties of the VBM charge densities, whereas the CBM densities remain almost unchanged. This is to be expected because the hole occupies the VBM. Hole injection redistributes the VBM charge density over new regions of space in both VIV and VIP systems, which enhances the overlap with the CBM and prolongs the VBM-CBM coherence. The changes in the VBM properties can be attributed to the following two aspects. First, the hole injection induces a Pb-I lattice distortion, particularly in VIV. Because the VBM arises from overlapping Pb-6s and I-5p orbitals, it is more sensitive than the CBM to the distortion of the Pb-I lattice. Hence, the hole has a stronger influence on the charge distribution of the VBM than the CBM. Second, the injected hole can change the charge distribution of the VBM by varying the electrostatic potential. Previous work⁶⁸ has reported that the electrostatic potential fluctuation can significantly shift the VBM energy level and alter its charge localization. The fluctuation in the electrostatic potential is closely related with the configuration and the local electric field induced by MA dipoles. The injected hole can change both the configuration and the inner electric field. Figure 4e,j shows a considerable difference in the electrostatic potentials of the hole-free and hole-injected perovskites. The main difference happens exactly where the new charge density of the VBM appears, Z from 2.5 to 5 Å, which directly confirms our conclusion. Once again,

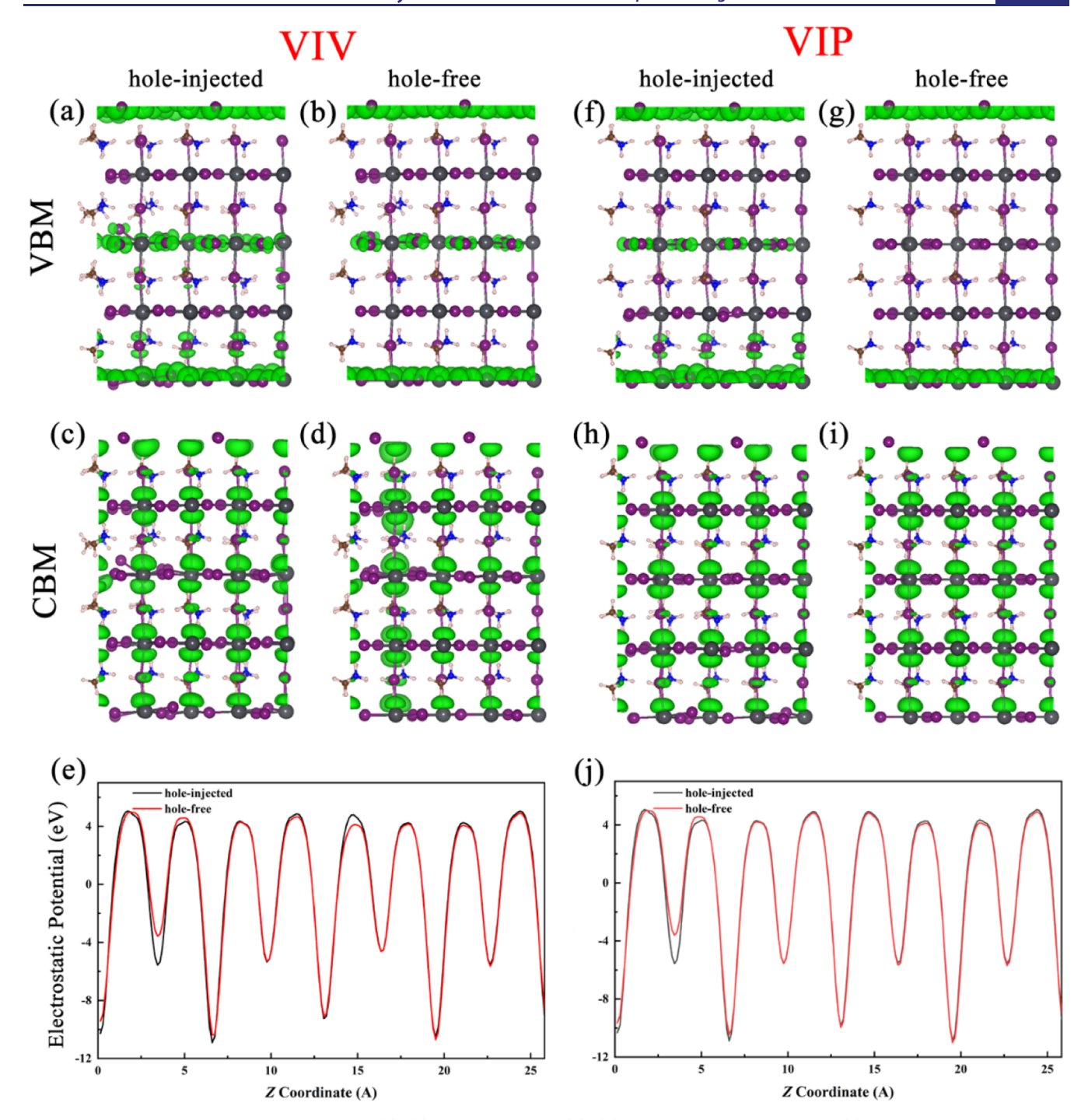


Figure 4. Charge densities of the VBM/CBM in (a)/(c) hole-injected and (b)/(d) hole-free VIV perovskite, and (e) electrostatic potential of the hole-injected and hole-free VIV systems. (f-j) Corresponding results for the VIP perovskite.

VIV shows a larger potential difference because the hole in VIV induces a more serious configuration distortion. Thus, the hole injection accelerates the nonradiative recombination mainly by prolonging the pure-dephasing time.

It should be noted that the NAMD of this work reveals the synergy between the hole injection and the nonradiative e—h recombination, whereas no iodine migration process has been captured after the hole injection in MD simulations. At the same time, both our simulations and experimental results have indicated clearly that the hole injection can greatly accelerate the ion migration. Thus, hole trapping, ion migration, and charge carrier recombination are all coupled in metal halide

perovskites, exhibiting notable synergetic behavior. Only iodine ion migration has been considered in the current work due to its lowest migration barriers and because iodine vacancy is the most stable native defect with the lowest formation energy. Migration of other ions, such as Pb²⁺ and MA⁺, can also influence the charge carrier lifetimes, and at the same time, the ion migration can be influenced by charge injection. Migration of Pb can be particularly important because similar to I, Pb contributes to the band edge and because charge injection induces distortion in the Pb–I lattice. Although the current work focuses on the MAPbI₃ perovskite, the general conclusions should hold for other perovskites,

provided they exhibit similar lattice softness and ion mobility. Particularly, the interplay between charge injection and ion migration may follow different mechanisms in all-inorganic perovskites, such as CsPbI₃, because they are typically stiffer and lack asymmetric MA-type cations whose orientation plays an important role in the ion migration. The synergy between charge injection, trapping and recombination, and ion migration constitutes an important topic requiring further studies.

4. CONCLUSIONS

In summary, using ab initio time-independent and real-time time-dependent DFT, coupled with NAMD, we have investigated iodine vacancy migration and nonradiative e-h recombination in the hole-free and hole-injected MAPbI₃ perovskites. We demonstrated that the injected hole can induce a Pb-I lattice distortion, especially when the iodine vacancy is located at the vertical site, namely the top or bottom site of the PbI₆ octahedron along the Z direction. The iodine diffusion is accelerated for two reasons. The diffusion energy barrier in the XY plane is significantly decreased, and the migration length in the vertical (Z) direction is shortened due to a significant lattice distortion. Because ion migration accelerates the nonradiative recombination, the hole injection accelerates the recombination by promoting the migration. The analysis also shows that the hole injection strengthens electron-phonon interactions related with Pb-I lattice motions. Compared with the CBM, the VBM of MAPbI3 is much more sensitive to the hole. The enhanced CBM-VBM overlap in the presence of the hole extends quantum coherence between the initial and final states. The accelerated ion migration, the increased electron-phonon interaction, and the extended coherence time act together to boost the e-h recombination after the hole injection. Our work suggests strongly that high concentration of holes should be inhibited in perovskites because holes promote ion migration and shorten charge carrier lifetimes. The in-depth understanding of the synergy among hole trapping, ion migration, and charge carrier recombination generated by our simulations is essential for designing high efficiency perovskite solar cells and other optoelectronic devices.

ASSOCIATED CONTENT

Supporting Information

The Supporting Information is available free of charge at https://pubs.acs.org/doi/10.1021/jacs.2c02148.

Densities of states of hole-injected perovskites and energy barriers and internal parameters for an alternative description of the hole (PDF)

AUTHOR INFORMATION

Corresponding Authors

Li-Min Liu — School of Physics, Beihang University, Beijing 100191, China; orcid.org/0000-0003-3925-5310; Email: liminliu@buaa.edu.cn

Oleg V. Prezhdo — Department of Chemistry, University of Southern California, Los Angeles, California 90089, United States; ocid.org/0000-0002-5140-7500;

Email: prezhdo@usc.edu

Authors

Chuan-Jia Tong — Hunan Key Laboratory of Nanophotonics and Devices, Hunan Key Laboratory of Super-Microstructure and Ultrafast Process, School of Physics and Electronics, Central South University, Changsha 410083, China; orcid.org/0000-0001-6554-5827

Xiaoyi Cai – School of Physics, Beihang University, Beijing 100191, China

An-Yu Zhu — Hunan Key Laboratory of Nanophotonics and Devices, Hunan Key Laboratory of Super-Microstructure and Ultrafast Process, School of Physics and Electronics, Central South University, Changsha 410083, China

Complete contact information is available at: https://pubs.acs.org/10.1021/jacs.2c02148

Notes

The authors declare no competing financial interest.

ACKNOWLEDGMENTS

This work was supported by the National Natural Science Foundation of China (nos. 12104515, 11974037 and 51861130360), the Royal Society Newton Advanced Fellowships (no. NAF\R1\180242), and the U.S. National Science Foundation (grant no. CHE-2154367). O.V.P. acknowledges support of the US Department of Energy (grant no. DE-SC0014429). We acknowledge Dr. W.-T. Wang from the University of York for helpful discussion. We are grateful for resources from the High Performance Computing Center of Central South University. We also acknowledge the computational support from HPC of the Beihang University.

REFERENCES

- (1) Bag, M.; Renna, L. A.; Adhikari, R. Y.; Karak, S.; Liu, F.; Lahti, P. M.; Russell, T. P.; Tuominen, M. T.; Venkataraman, D. Kinetics of Ion Transport in Perovskite Active Layers and Its Implications for Active Layer Stability. *J. Am. Chem. Soc.* **2015**, *137*, 13130.
- (2) Kamat, P. V.; Kuno, M. Halide Ion Migration in Perovskite Nanocrystals and Nanostructures. *Acc. Chem. Res.* **2021**, *54*, 520.
- (3) Liu, Y.; Ievlev, A. V.; Borodinov, N.; Lorenz, M.; Xiao, K.; Ahmadi, M.; Hu, B.; Kalinin, S. V.; Ovchinnikova, O. S. Direct Observation of Photoinduced Ion Migration in Lead Halide Perovskites. *Adv. Funct. Mater.* **2021**, *31*, 2008777.
- (4) Li, M.; Han, S.; Liu, Y.; Luo, J.; Hong, M.; Sun, Z. Soft Perovskite-Type Antiferroelectric with Giant Electrocaloric Strength near Room Temperature. *J. Am. Chem. Soc.* **2020**, *142*, 20744.
- (5) Ma, Y.; Cheng, Y.; Xu, X.; Li, M.; Zhang, C.; Cheung, S. H.; Zeng, Z.; Shen, D.; Xie, Y. M.; Chiu, K. L.; Lin, F.; So, S. K.; Lee, C. S.; Tsang, S. W. Suppressing Ion Migration across Perovskite Grain Boundaries by Polymer Additives. *Adv. Funct. Mater.* **2021**, *31*, 2006802.
- (6) Haruyama, J.; Sodeyama, K.; Han, L.; Tateyama, Y. First-Principles Study of Ion Diffusion in Perovskite Solar Cell Sensitizers. *J. Am. Chem. Soc.* **2015**, *137*, 10048.
- (7) Eames, C.; Frost, J. M.; Barnes, P. R. F.; O'Regan, B. C.; Walsh, A.; Islam, M. S. Ionic Transport in Hybrid Lead Iodide Perovskite Solar Cells. *Nat. Commun.* **2015**, *6*, 7497.
- (8) Yang, J.-H.; Yin, W.-J.; Park, J.-S.; Wei, S.-H. Fast Self-Diffusion of Ions in CH₃NH₃PbI₃: The Interstiticaly Mechanism Versus Vacancy-Assisted Mechanism. *J. Mater. Chem. A* **2016**, *4*, 13105.
- (9) Azpiroz, J. M.; Mosconi, E.; Bisquert, J.; De Angelis, F. Defect Migration in Methylammonium Lead Iodide and Its Role in Perovskite Solar Cell Operation. *Energy Environ. Sci.* **2015**, 8, 2118.
- (10) Yuan, Y.; Wang, Q.; Shao, Y.; Lu, H.; Li, T.; Gruverman, A.; Huang, J. Electric-Field-Driven Reversible Conversion between

- Methylammonium Lead Triiodide Perovskites and Lead Iodide at Elevated Temperatures. *Adv. Energy Mater.* **2016**, *6*, 1501803.
- (11) Elmelund, T.; Scheidt, R. A.; Seger, B.; Kamat, P. V. Bidirectional Halide Ion Exchange in Paired Lead Halide Perovskite Films with Thermal Activation. ACS Energy Lett. 2019, 4, 1961.
- (12) Lin, D.; Shi, T.; Xie, H.; Wan, F.; Ren, X.; Liu, K.; Zhao, Y.; Ke, L.; Lin, Y.; Gao, Y.; Xu, X.; Xie, W.; Liu, P.; Yuan, Y. Ion Migration Accelerated Reaction between Oxygen and Metal Halide Perovskites in Light and Its Suppression by Cesium Incorporation. *Adv. Energy Mater.* **2021**, *11*, 2002552.
- (13) Cui, S.; Wang, J.; Xie, H.; Zhao, Y.; Li, Z.; Luo, S.; Ke, L.; Gao, Y.; Meng, K.; Ding, L.; Yuan, Y. Rubidium Ions Enhanced Crystallinity for Ruddlesden—Popper Perovskites. *Adv. Sci.* **2020**, *7*, 2002445.
- (14) Richardson, G.; O'Kane, S. E. J.; Niemann, R. G.; Peltola, T. A.; Foster, J. M.; Cameron, P. J.; Walker, A. B. Can Slow-Moving Ions Explain Hysteresis in the Current-Voltage Curves of Perovskite Solar Cells? *Energy Environ. Sci.* **2016**, *9*, 1476.
- (15) Son, D.-Y.; Kim, S.-G.; Seo, J.-Y.; Lee, S.-H.; Shin, H.; Lee, D.; Park, N.-G. Universal Approach toward Hysteresis-Free Perovskite Solar Cell Via Defect Engineering. *J. Am. Chem. Soc.* **2018**, *140*, 1358.
- (16) van Reenen, S.; Kemerink, M.; Snaith, H. J. Modeling Anomalous Hysteresis in Perovskite Solar Cells. *J. Phys. Chem. Lett.* **2015**, *6*, 3808.
- (17) Chen, R.; Cao, J.; Duan, Y.; Hui, Y.; Chuong, T. T.; Ou, D.; Han, F.; Cheng, F.; Huang, X.; Wu, B.; Zheng, N. High-Efficiency, Hysteresis-Less, UV-Stable Perovskite Solar Cells with Cascade ZnO–ZnS Electron Transport Layer. J. Am. Chem. Soc. 2019, 141, 541.
- (18) Tong, C.-J.; Li, L.; Liu, L.-M.; Prezhdo, O. V. Synergy between Ion Migration and Charge Carrier Recombination in Metal-Halide Perovskites. *J. Am. Chem. Soc.* **2020**, *142*, 3060.
- (19) Kim, Y.-H.; Wolf, C.; Kim, H.; Lee, T.-W. Charge Carrier Recombination and Ion Migration in Metal-Halide Perovskite Nanoparticle Films for Efficient Light-Emitting Diodes. *Nano Energy* **2018**, *52*, 329.
- (20) Gerhard, M.; Louis, B.; Camacho, R.; Merdasa, A.; Li, J.; Kiligaridis, A.; Dobrovolsky, A.; Hofkens, J.; Scheblykin, I. G. Microscopic Insight into Non-Radiative Decay in Perovskite Semiconductors from Temperature-Dependent Luminescence Blinking. *Nat. Commun.* **2019**, *10*, 1698.
- (21) Stranks, S. D. Nonradiative Losses in Metal Halide Perovskites. *ACS Energy Lett.* **2017**, *2*, 1515.
- (22) Walsh, A.; Stranks, S. D. Taking Control of Ion Transport in Halide Perovskite Solar Cells. ACS Energy Lett. 2018, 3, 1983.
- (23) Samu, G. F.; Balog, A.; De Angelis, F.; Meggiolaro, D.; Kamat, P. V.; Janáky, C. Electrochemical Hole Injection Selectively Expels Iodide from Mixed Halide Perovskite Films. *J. Am. Chem. Soc.* **2019**, 141, 10812.
- (24) DuBose, J. T.; Kamat, P. V. TiO₂-Assisted Halide Ion Segregation in Mixed Halide Perovskite Films. *J. Am. Chem. Soc.* **2020**, *142*, 5362.
- (25) Xiao, X.; Wang, K.; Ye, T.; Cai, R.; Ren, Z.; Wu, D.; Qu, X.; Sun, J.; Ding, S.; Sun, X. W.; Choy, W. C. H. Enhanced Hole Injection Assisted by Electric Dipoles for Efficient Perovskite Light-Emitting Diodes. *Commun. Mater.* **2020**, *1*, 81.
- (26) VandeVondele, J.; Hutter, J. Gaussian Basis Sets for Accurate Calculations on Molecular Systems in Gas and Condensed Phases. *J. Chem. Phys.* **2007**, *127*, 114105.
- (27) VandeVondele, J.; Krack, M.; Mohamed, F.; Parrinello, M.; Chassaing, T.; Hutter, J. Quickstep: Fast and Accurate Density Functional Calculations Using a Mixed Gaussian and Plane Waves Approach. *Comput. Phys. Commun.* **2005**, *167*, 103.
- (28) Goedecker, S.; Teter, M.; Hutter, J. Separable Dual-Space Gaussian Pseudopotentials. *Phys. Rev. B: Condens. Matter Mater. Phys.* **1996**, *54*, 1703.
- (29) Perdew, J. P.; Burke, K.; Ernzerhof, M. Generalized Gradient Approximation Made Simple. *Phys. Rev. Lett.* **1996**, *77*, 3865.

- (30) He, J.; Fang, W.-H.; Long, R.; Prezhdo, O. V. Bidentate Lewis Bases Are Preferred for Passivation of MAPbI₃ Surfaces: A Time-Domain Ab Initio Analysis. *Nano Energy* **2021**, *79*, 105491.
- (31) Li, W.; Zhan, J.; Liu, X.; Tang, J.; Yin, W.-J.; Prezhdo, O. V. Atomistic Mechanism of Passivation of Halide Vacancies in Lead Halide Perovskites by Alkali Ions. *Chem. Mater.* **2021**, 33, 1285.
- (32) Tong, C.-J.; Geng, W.; Tang, Z.-K.; Yam, C.-Y.; Fan, X.-L.; Liu, J.; Lau, W.-M.; Liu, L.-M. Uncovering the Veil of the Degradation in Perovskite CH₃NH₃PbI₃ Upon Humidity Exposure: A First-Principles Study. *J. Phys. Chem. Lett.* **2015**, *6*, 3289.
- (33) Aristidou, N.; Eames, C.; Sanchez-Molina, I.; Bu, X.; Kosco, J.; Islam, M. S.; Haque, S. A. Fast Oxygen Diffusion and Iodide Defects Mediate Oxygen-Induced Degradation of Perovskite Solar Cells. *Nat. Commun.* **2017**, *8*, 15218.
- (34) Li, W.; Sun, Y.-Y.; Li, L.; Zhou, Z.; Tang, J.; Prezhdo, O. V. Control of Charge Recombination in Perovskites by Oxidation State of Halide Vacancy. *J. Am. Chem. Soc.* **2018**, *140*, 15753.
- (35) Grimme, S.; Antony, J.; Ehrlich, S.; Krieg, H. A Consistent and Accurate Ab Initio Parametrization of Density Functional Dispersion Correction (DFT-D) for the 94 Elements H-Pu. *J. Chem. Phys.* **2010**, 132, 154104.
- (36) Grimme, S.; Ehrlich, S.; Goerigk, L. Effect of the Damping Function in Dispersion Corrected Density Functional Theory. *J. Comput. Chem.* **2011**, 32, 1456.
- (37) Henkelman, G.; Uberuaga, B. P.; Jónsson, H. A Climbing Image Nudged Elastic Band Method for Finding Saddle Points and Minimum Energy Paths. *J. Chem. Phys.* **2000**, *113*, 9901.
- (38) Henkelman, G.; Jónsson, H. Improved Tangent Estimate in the Nudged Elastic Band Method for Finding Minimum Energy Paths and Saddle Points. *J. Chem. Phys.* **2000**, *113*, 9978.
- (39) Jaeger, H. M.; Fischer, S.; Prezhdo, O. V. Decoherence-Induced Surface Hopping. *J. Chem. Phys.* **2012**, *137*, 22A545.
- (40) Akimov, A. V.; Prezhdo, O. V. The Pyxaid Program for Non-Adiabatic Molecular Dynamics in Condensed Matter Systems. *J. Chem. Theory Comput.* **2013**, *9*, 4959.
- (41) Akimov, A. V.; Prezhdo, O. V. Advanced Capabilities of the Pyxaid Program: Integration Schemes, Decoherence Effects, Multi-excitonic States, and Field-Matter Interaction. *J. Chem. Theory Comput.* **2014**, *10*, 789.
- (42) Prezhdo, O. V. Modeling Non-Adiabatic Dynamics in Nanoscale and Condensed Matter Systems. *Acc. Chem. Res.* **2021**, 54, 4239.
- (43) Li, W.; She, Y.; Vasenko, A. S.; Prezhdo, O. V. Ab Initio Nonadiabatic Molecular Dynamics of Charge Carriers in Metal Halide Perovskites. *Nanoscale* **2021**, *13*, 10239.
- (44) Zhou, G.; Lu, G.; Prezhdo, O. V. Modeling Auger Processes with Nonadiabatic Molecular Dynamics. *Nano Lett.* **2021**, *21*, 756.
- (45) Sarkar, R.; Kar, M.; Habib, M.; Zhou, G.; Frauenheim, T.; Sarkar, P.; Pal, S.; Prezhdo, O. V. Common Defects Accelerate Charge Separation and Reduce Recombination in CNT/Molecule Composites: Atomistic Quantum Dynamics. J. Am. Chem. Soc. 2021, 143, 6649
- (46) Cheng, C.; Fang, W.-H.; Long, R.; Prezhdo, O. V. Water Splitting with a Single-Atom Cu/TiO_2 Photocatalyst: Atomistic Origin of High Efficiency and Proposed Enhancement by Spin Selection. *JACS Au* **2021**, *1*, 550.
- (47) Chu, W.; Saidi, W. A.; Prezhdo, O. V. Long-Lived Hot Electron in a Metallic Particle for Plasmonics and Catalysis: Ab Initio Nonadiabatic Molecular Dynamics with Machine Learning. *ACS Nano* **2020**, *14*, 10608.
- (48) Li, L.; Long, R.; Bertolini, T.; Prezhdo, O. V. Sulfur Adatom and Vacancy Accelerate Charge Recombination in MoS₂ but by Different Mechanisms: Time-Domain Ab Initio Analysis. *Nano Lett.* **2017**, *17*, 7962.
- (49) Akimov, A. V.; Asahi, R.; Jinnouchi, R.; Prezhdo, O. V. What Makes the Photocatalytic CO_2 Reduction on N-Doped $\mathrm{Ta}_2\mathrm{O}_5$ Efficient: Insights from Nonadiabatic Molecular Dynamics. *J. Am. Chem. Soc.* **2015**, *137*, 11517.

- (50) Stier, W.; Duncan, W. R.; Prezhdo, O. V. Thermally Assisted Sub-10 Fs Electron Transfer in Dye-Sensitized Nanocrystalline TiO₂ Solar Cells. *Adv. Mater.* **2004**, *16*, 240.
- (51) Tong, C.-J.; Geng, W.; Prezhdo, O. V.; Liu, L.-M. Role of Methylammonium Orientation in Ion Diffusion and Current–Voltage Hysteresis in the CH₃NH₃PbI₃ Perovskite. *ACS Energy Lett.* **2017**, *2*, 1997
- (52) Rutter, M. J. Charged Surfaces and Slabs in Periodic Boundary Conditions. *Electron. Struct.* **2021**, *3*, 015002.
- (53) Schlipf, M.; Poncé, S.; Giustino, F. Carrier Lifetimes and Polaronic Mass Enhancement in the Hybrid Halide Perovskite CH₃NH₃PbI₃ from Multiphonon Frohlich Coupling. *Phys. Rev. Lett.* **2018**, *121*, 086402.
- (54) Chu, W.; Zheng, Q.; Prezhdo, O. V.; Zhao, J.; Saidi, W. A. Low-Frequency Lattice Phonons in Halide Perovskites Explain High Defect Tolerance toward Electron-Hole Recombination. *Sci. Adv.* **2020**, *6*, No. eaaw7453.
- (55) Poncé, S.; Schlipf, M.; Giustino, F. Origin of Low Carrier Mobilities in Halide Perovskites. ACS Energy Lett. 2019, 4, 456.
- (56) Miyata, K.; Meggiolaro, D.; Trinh, M. T.; Joshi, P. P.; Mosconi, E.; Jones, S. C.; De Angelis, F.; Zhu, X. Y. Large Polarons in Lead Halide Perovskites. *Sci. Adv.* **2017**, *3*, No. e1701217.
- (57) Zhang, Z.; Long, R.; Tokina, M. V.; Prezhdo, O. V. Interplay between Localized and Free Charge Carriers Can Explain Hot Fluorescence in the CH₃NH₃PbBr₃ Perovskite: Time-Domain Ab Initio Analysis. *J. Am. Chem. Soc.* **2017**, *139*, 17327.
- (58) Zhou, Z.; Long, R.; Prezhdo, O. V. Why Silicon Doping Accelerates Electron Polaron Diffusion in Hematite. *J. Am. Chem. Soc.* **2019**, *141*, 20222.
- (59) Liao, P.; Carter, E. A. Hole Transport in Pure and Doped Hematite. *J. Appl. Phys.* **2012**, *112*, 013701.
- (60) Ansari, N.; Ulman, K.; Camellone, M. F.; Seriani, N.; Gebauer, R.; Piccinin, S. Hole Localization in Fe_2O_3 from Density Functional Theory and Wave-Function-Based Methods. *Phys. Rev. Mater.* **2017**, 1, 035404.
- (61) Mahata, A.; Meggiolaro, D.; De Angelis, F. From Large to Small Polarons in Lead, Tin, and Mixed Lead—Tin Halide Perovskites. *J. Phys. Chem. Lett.* **2019**, *10*, 1790.
- (62) Chu, W.; Saidi, W. A.; Zhao, J.; Prezhdo, O. V. Soft Lattice and Defect Covalency Rationalize Tolerance of β -CsPbI $_3$ Perovskite Solar Cells to Native Defects. *Angew. Chem., Int. Ed.* **2020**, *59*, 6435.
- (63) Zhou, G.; Chu, W.; Prezhdo, O. V. Structural Deformation Controls Charge Losses in MAPbI₃: Unsupervised Machine Learning of Nonadiabatic Molecular Dynamics. ACS Energy Lett. 2020, 5, 1930.
- (64) Quarti, C.; Grancini, G.; Mosconi, E.; Bruno, P.; Ball, J. M.; Lee, M. M.; Snaith, H. J.; Petrozza, A.; De Angelis, F. The Raman Spectrum of the CH₃NH₃PbI₃ Hybrid Perovskite: Interplay of Theory and Experiment. *J. Phys. Chem. Lett.* **2014**, *5*, 279.
- (65) Tong, C.-J.; Li, L.; Liu, L.-M.; Prezhdo, O. V. Long Carrier Lifetimes in PbI₂-Rich Perovskites Rationalized by Ab Initio Nonadiabatic Molecular Dynamics. *ACS Energy Lett.* **2018**, *3*, 1868.
- (66) Zhang, Z.; Qiao, L.; Mora-Perez, C.; Long, R.; Prezhdo, O. V. Pb Dimerization Greatly Accelerates Charge Losses in MAPbI₃: Time-Domain Ab Initio Analysis. *J. Chem. Phys.* **2020**, *152*, 064707.
- (67) Li, W.; Chen, Z.; Tang, J.; Prezhdo, O. V. Anti-Correlation between Band Gap and Carrier Lifetime in Lead Halide Perovskites under Compression Rationalized by Ab Initio Quantum Dynamics. *Chem. Mater.* **2020**, 32, 4707.
- (68) Geng, W.; Hu, Q.; Tong, C. J.; Tang, Z. K.; Liu, L. M. The Influence of Dipole Moments Induced by Organic Molecules and Domain Structures on the Properties of CH₃NH₃PbI₃ Perovskite. *Adv. Theory Simul.* **2019**, *2*, 1900041.

□ Recommended by ACS

Persistent Ion Accumulation at Interfaces Improves the Performance of Perovskite Solar Cells

Joshua A. Kress, Yana Vaynzof, et al.

SEPTEMBER 07, 2022 ACS ENERGY LETTERS

READ 🗹

Structural Disorder in Higher-Temperature Phases Increases Charge Carrier Lifetimes in Metal Halide Perovskites

Ran Shi, Oleg V. Prezhdo, et al.

OCTOBER 07, 2022

JOURNAL OF THE AMERICAN CHEMICAL SOCIETY

READ 🗹

Tuning Defects in a Halide Double Perovskite with Pressure

Nathan R. Wolf, Hemamala I. Karunadasa, et al.

NOVEMBER 07, 2022

JOURNAL OF THE AMERICAN CHEMICAL SOCIETY

READ 🗹

Suppressing Oxygen-Induced Deterioration of Metal Halide Perovskites by Alkaline Earth Metal Doping: A Quantum Dynamics Study

Lu Qiao, Run Long, et al.

MARCH 16, 2022

JOURNAL OF THE AMERICAN CHEMICAL SOCIETY

READ **C**

Get More Suggestions >